

RESEARCH ARTICLE

High-throughput interaction screens illuminate the role of c-di-AMP in cyanobacterial nighttime survival

Benjamin E. Rubin¹, TuAnh Ngoc Huynh², David G. Welkie³, Spencer Diamond¹, Ryan Simkovsky³, Emily C. Pierce¹, Arnaud Taton¹, Laura C. Lowe³, Jenny J. Lee¹, Scott A. Rifkin¹, Joshua J. Woodward², Susan S. Golden^{1,3*}

1 Division of Biological Sciences, University of California San Diego, La Jolla, CA, United States of America, **2** Department of Microbiology, University of Washington, Seattle, WA, United States of America, **3** Center for Circadian Biology, University of California San Diego, La Jolla, CA, United States of America

* sgolden@ucsd.edu



OPEN ACCESS

Citation: Rubin BE, Huynh TN, Welkie DG, Diamond S, Simkovsky R, Pierce EC, et al. (2018) High-throughput interaction screens illuminate the role of c-di-AMP in cyanobacterial nighttime survival. *PLoS Genet* 14(4): e1007301. <https://doi.org/10.1371/journal.pgen.1007301>

Editor: Mark Gomelsky, University of Wyoming, UNITED STATES

Received: August 21, 2017

Accepted: March 8, 2018

Published: April 2, 2018

Copyright: © 2018 Rubin et al. This is an open access article distributed under the terms of the [Creative Commons Attribution License](https://creativecommons.org/licenses/by/4.0/), which permits unrestricted use, distribution, and reproduction in any medium, provided the original author and source are credited.

Data Availability Statement: All relevant data are within the paper and its Supporting Information files.

Funding: This work was supported by research grants (R01AI116669 to JJW; R35GM118290 to SSG) and training grants (5T32AI055396 to TNH; T32GM007240 to BER and SD) from the National Institutes of Health; a grant from the Pew Charitable Trust (to JJW); and grants from the National Science Foundation (MCB1517482 to SAR; MCB1244108 and IOS1322808 to SSG). The

Abstract

The broadly conserved signaling nucleotide cyclic di-adenosine monophosphate (c-di-AMP) is essential for viability in most bacteria where it has been studied. However, characterization of the cellular functions and metabolism of c-di-AMP has largely been confined to the class Bacilli, limiting our functional understanding of the molecule among diverse phyla. We identified the cyclase responsible for c-di-AMP synthesis and characterized the molecule's role in survival of darkness in the model photosynthetic cyanobacterium *Synechococcus elongatus* PCC 7942. In addition to the use of traditional genetic, biochemical, and proteomic approaches, we developed a high-throughput genetic interaction screen (IRB-Seq) to determine pathways where the signaling nucleotide is active. We found that in *S. elongatus* c-di-AMP is produced by an enzyme of the diadenylate cyclase family, CdaA, which was previously unexplored experimentally. A *cdaA*-null mutant experiences increased oxidative stress and death during the nighttime portion of day-night cycles, in which potassium transport is implicated. These findings suggest that c-di-AMP is biologically active in cyanobacteria and has non-canonical roles in the phylum including oxidative stress management and day-night survival. The pipeline and analysis tools for IRB-Seq developed for this study constitute a quantitative high-throughput approach for studying genetic interactions.

Author summary

Cyclic di-adenosine monophosphate (c-di-AMP) is a molecule that has significant roles in many microorganisms. This work shows the existence of c-di-AMP for the first time in photosynthetic microorganisms, cyanobacteria, and demonstrates its role in survival during the light-to-dark shifts that occur in day-night cycles. Despite the obvious importance of adaptation to these daily cycles for organisms that are fundamentally reliant on light, such as cyanobacteria, understanding of diurnal physiology is lacking because most cyanobacterial research is conducted during growth in constant light. To identify other

fundamental role in study design, data collection and analysis, decision to publish, or preparation of the manuscript.

Competing interests: The authors have declared that no competing interests exist.

players in c-di-AMP's function we developed a low-cost and efficient method for finding interactions between genes. The technique combines one mutation, in this case for the gene that encodes the enzyme for synthesis of c-di-AMP, with thousands of other individual mutations to find pairwise interactions that affect fitness of the resulting mutants. Mutants are tagged with DNA barcodes to allow their survival to be easily tracked in a population of cells. The method enables us to place the function of c-di-AMP within the context of pathways previously known to be involved in day-night survival. Taken together, this work expands the known roles of c-di-AMP, improves our understanding of cyanobacterial survival in day-night cycles, and presents an improved approach for determining genetic interactions.

Introduction

The signaling nucleotide cyclic di-adenosine monophosphate (c-di-AMP) has been implicated in a wide range of biological processes since its discovery less than a decade ago [1]. The molecule is active in multiple pathways including potassium transport, regulation of central metabolism, cell wall homeostasis, gene expression, and DNA damage responses [2]. In addition, c-di-AMP is the only second messenger that is essential to most of the organisms in which it is studied [3]. Despite the biological importance of c-di-AMP, *in vivo* studies of this signaling nucleotide have focused on a narrow array of Firmicutes and to a lesser extent Actinobacteria. Expanding the investigation of c-di-AMP to a broader diversity of microbial phyla may reveal new functions for this molecule.

Organisms in the photosynthetic phylum Cyanobacteria are key players in global carbon, oxygen, and nitrogen cycling, and are promising platforms for renewable production of industrial chemicals [4–6]. While c-di-AMP has not been reported in the phylum, the existence of enzymes and riboswitches predicted by homology to interact with the molecule suggests its presence [2,7–9]. Signaling nucleotides previously studied in cyanobacteria (cGMP, c-di-GMP, (p)ppGpp, and cAMP) serve important roles in environmental responses and have revealed activities specific to photosynthetic organisms, such as regulating phototaxis, photosystem repair, and dark survival [8,10]. Characterization of c-di-AMP metabolism and its role in cyanobacteria may similarly lead to a better understanding of the phylum, as well as the functions of c-di-AMP.

C-di-AMP research, as a young field with many unknowns, has particularly benefited from untargeted genetic interaction screens. Screens focused on secondary mutations that relieve the phenotypes of c-di-AMP-related mutants (alleviating interactions) have successfully identified genetic interactions with c-di-AMP synthases and phosphodiesterases [11,12]. However, these screens have been limited to assaying positive interactions, were non-quantitative, and have been performed under only a single condition.

Quantitative genetic interaction screens to identify aggravating as well as alleviating interactions would provide a powerful tool to elucidate c-di-AMP function. Such screens have been conducted for other processes using next-generation sequencing paired with transposon mutagenesis (Tn-Seq) [13–15]. Tn-Seq for genetic interactions relies upon the generation of a new mutant library for each screen in the background of a knockout of interest [16]. While informative, the need to generate and characterize a new transposon-mutant library for each interaction screen is both costly and labor intensive [17]. These features have limited the applicability of Tn-Seq for interaction screens. A variation on Tn-Seq, RB-TnSeq, provides a cheaper and less laborious approach for screening transposon mutant libraries, in which the fitness of mutants

in the population is tracked by sequencing and counting of 20-base pair “barcodes” in each transposon [18]. This approach has not yet been applied to interaction screens, where it offers great potential for mitigating their logistical weaknesses and enlarging their scope.

Here, we used genetic and biochemical approaches to elucidate the presence and roles of c-di-AMP in the cyanobacterium *Synechococcus elongatus* PCC 7942. To further probe the molecule’s functions we developed and implemented an approach we named interaction RB-TnSeq, or IRB-Seq, to quantitatively measure genetic interactions with the c-di-AMP cyclase under multiple conditions.

Results

Presence of c-di-AMP and its cyclase

The putative c-di-AMP-producing and degrading enzymes in *S. elongatus* were identified computationally. Two domain organizations, DHH-DHHA1 (PF01368 and PF02272) and 7TM-7TMR_HD (PF07698), have been found to degrade c-di-AMP [19]. The software package HMMER [20] identified one of each in *S. elongatus*. Based on homology, the DHH-DHHA1 domain-containing protein, RecJ (Synpcc7942_1886), likely serves as a single-stranded DNA exonuclease. However, it may also act as a non-specific phosphodiesterase for c-di-AMP and linear 5'-phospho diadenylate (pApA), as documented in the literature [19]. The 7TM-7TMR_HD-containing protein, Synpcc7942_0779, is a reciprocal best hit with the *Listeria monocytogenes* c-di-AMP degrading enzyme PgpH, with homology focused around the HD domain active site. Therefore, Synpcc7942_0779, and to a lesser extent RecJ, are likely phosphodiesterases for c-di-AMP in *S. elongatus*.

A single protein in the organism contains a DisA_N domain (PF02457), currently the only domain known to be responsible for c-di-AMP production [21]. Although presence of this putative synthase has been noted several times in cyanobacteria, it has yet to be experimentally validated [2,8,9,22]. This sequence, annotated at time of publication as “protein of unknown function DUF147”, predicts three transmembrane segments and a cytoplasmic DisA_N domain (Fig 1A). The arrangement of domains identifies the protein as a member of the most abundant family of DisA_N domain-containing proteins, CdaA [2,23]. Thus, we refer to this previously unannotated gene, which encodes the putative cyclase of c-di-AMP, as *cdaA* (Synpcc7942_0263).

To validate this bioinformatic prediction of the c-di-AMP cyclase, we quantified c-di-AMP levels in wild type (WT) and a *cdaA*-null mutant using LC-MS. The WT value of 18.8 μM (Fig 1B) is higher than reported in other organisms, including *Staphylococcus aureus* [24] and *Bacillus subtilis* [25], where the nucleotide plays biologically important roles. While c-di-AMP is essential for many other c-di-AMP-producing organisms, a fully segregated insertion mutant for *cdaA*, which has no other paralog in the genome of *S. elongatus*, is viable under constant-light standard laboratory conditions (S1 Fig). The residual signal in the *cdaA* mutant, potentially attributable to c-di-AMP (Fig 1B), was within the background noise in mass spectrometry quantification and unlikely to represent presence of the molecule (S2 Fig). In further support of CdaA’s role in c-di-AMP synthesis, the *S. elongatus cdaA* was expressed in *Escherichia coli*, which does not naturally produce c-di-AMP; high levels of the molecule were detected (S3 Fig). These data strongly suggest that *S. elongatus* produces c-di-AMP, and that CdaA catalyzes its synthesis.

Concentrations of other signaling nucleotides studied in cyanobacteria change in response to light [8]. To investigate whether this may be the case with c-di-AMP in *S. elongatus*, we sampled every six hours over one 12-h light:12-h-dark cycle (LDC). The c-di-AMP concentration was variable in WT both among samples within time points and between them, with an apparent, although non-significant, trend upwards at nighttime (Fig 1C). Given that signaling

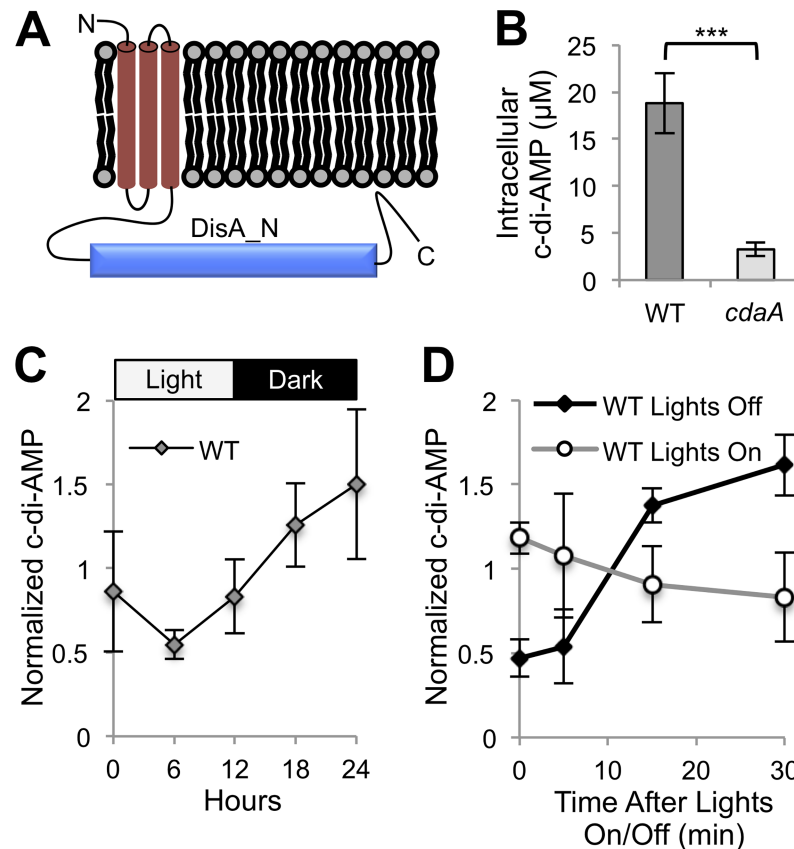


Fig 1. Presence, synthesis, and light-dependence of c-di-AMP in *S. elongatus*. (A) Predicted CdaA protein topology. (B) Intracellular c-di-AMP measured by LC-MS for WT and *cdaA* transposon mutant (8S16-L9). Intracellular c-di-AMP concentrations were determined from raw quantities using cell volume (see [Materials and Methods](#)). The error bars represent standard error (SE) of five time points taken throughout a 24-h LDC in quadruplicate. *** $P < 10^{-7}$ (Mann-Whitney-Wilcoxon Test). (C) C-di-AMP quantities in WT over one LDC. (D) C-di-AMP quantities upon the onset of darkness or light in WT. (C and D) C-di-AMP quantities are normalized by dividing by the average c-di-AMP concentration of the replicate. Error bars represent SE of four replicates.

<https://doi.org/10.1371/journal.pgen.1007301.g001>

nucleotide responses to light have been shown to occur within minutes in cyanobacteria [26], we performed higher resolution sampling around the light-to-dark and dark-to-light transitions. While light did not have a large or immediate effect on c-di-AMP, a three-fold increase in the nucleotide's levels was observed 15 minutes after onset of darkness (Fig 1D).

LDC sensitivity in *cdaA* mutant

Based on the observed increase in c-di-AMP levels upon onset of darkness, as well as previous research showing the importance of the closely linked signaling nucleotide ppGpp to dark survival in *S. elongatus* [10], we examined whether c-di-AMP is necessary to survive LDCs. In both solid and liquid media, the *cdaA* mutant has decreased growth in LDCs, but not in constant light (Fig 2A and 2B). This phenotype was successfully complemented by the addition of a WT copy of the *cdaA* gene to a neutral site (S4 Fig). Furthermore, although the *cdaA* mutant's absorbance spectrum was not significantly different from WT's before sensitizing LDCs, bleaching was apparent 30 h after the start of an LDC, and worsened thereafter (S5 Fig). Therefore, the *cdaA* mutation and the associated decrease of c-di-AMP levels are likely responsible for the LDC-specific deleterious phenotype.

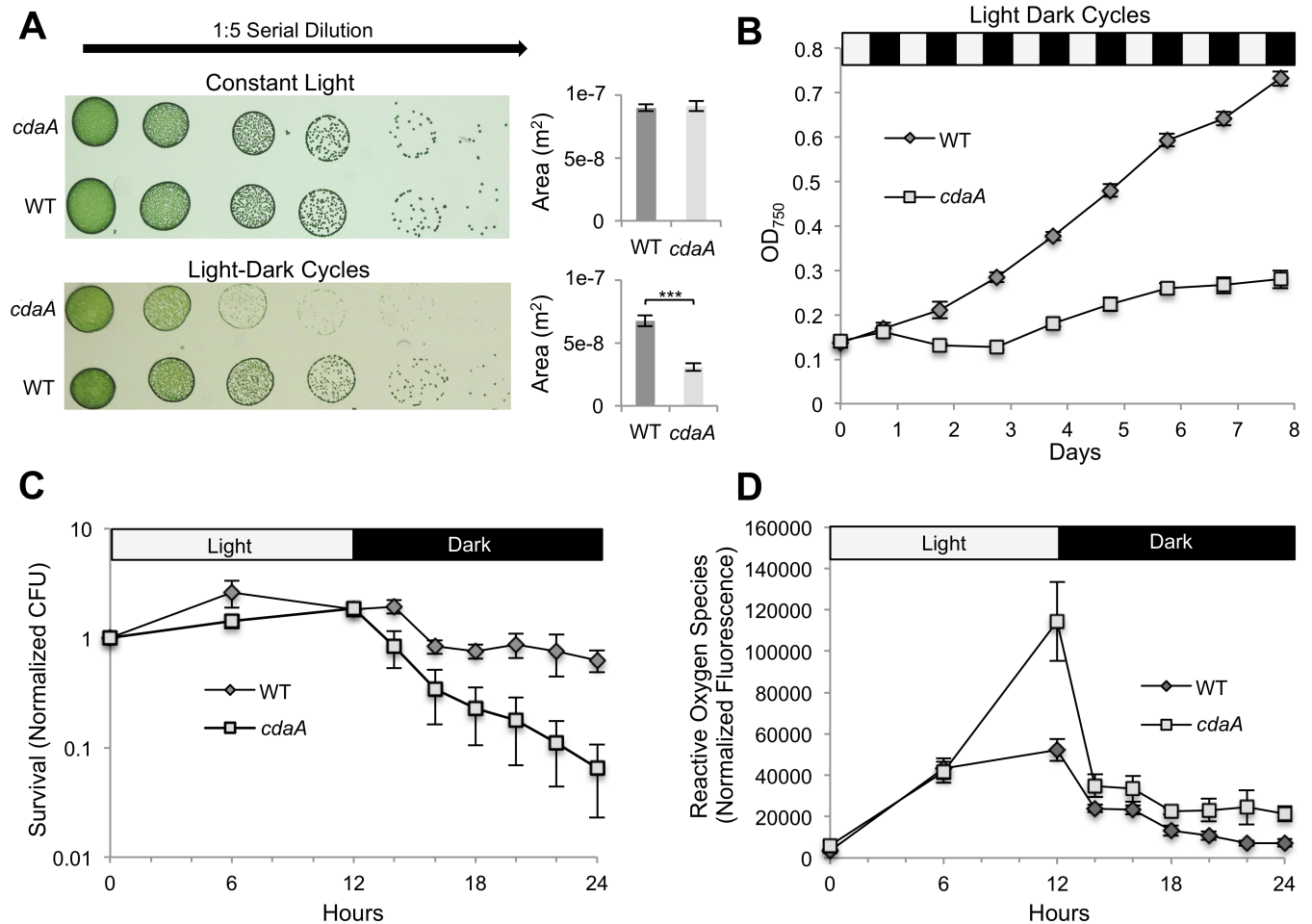


Fig 2. Sensitivity of *cdaA* mutant to LDCs. (A) Growth of WT and *cdaA* transposon mutant (8S16-L9) measured by spot plate under constant light and LDCs. ***P < 10⁻⁵ (Mann-Whitney-Wilcoxon Test). (B) Growth curve of WT and *cdaA* mutant in liquid culture in bioreactors under LDCs. (C) High resolution measurement of survival of WT and *cdaA* mutant throughout one LDC. Survival is quantified by CFU present at each time point normalized to CFU present at the first time point for each replicate. (D) ROS was measured by H2DCFDA fluorescence normalized by OD₇₅₀. Error bars in all figure parts indicate SE of four replicates.

<https://doi.org/10.1371/journal.pgen.1007301.g002>

To explore the nature and cause of the LDC sensitivity, we examined populations over one LDC. While the *cdaA* mutant grew similarly to WT over the light portion of the LDC, viability of the mutant, as measured by colony forming units in outgrowths in continuous light from specific time points, rapidly decreased upon the onset of darkness. This difference was significant after two hours of exposure to darkness (P < .05; *t* test), and became more pronounced over the course of the night (Fig 2C). Recent work showed that reactive oxygen species (ROS) correlate with death in darkness for *S. elongatus* [27]. Indeed, reactive oxygen species peaked in the mutant after the onset of darkness at more than two fold the level in WT and remained higher than WT through the course of the night (P < 10⁻⁵; Mann-Whitney-Wilcoxon Test) (Fig 2D). These data suggest that a still-cryptic mechanism actively kills the *cdaA* mutant specifically in the dark stage of the LDC and potentially as a consequence of high oxidative stress.

Genetic interactions of c-di-AMP

IRB-Seq design. The c-di-AMP signaling pathway is still enigmatic in cyanobacteria with no *in vivo* evidence that identifies other members of the pathway. Therefore, we used an

unbiased genome-wide approach to identify genes involved in c-di-AMP function through genetic interactions with c-di-AMP's cyclase, CdaA. The approach relied on a previously developed dense transposon insertion mutant library in *S. elongatus* [28]. Briefly, this library was built with the RB-TnSeq method [18], in which every loss-of-function mutant in the library contains a unique identifier sequence, or barcode (Fig 3A). By using next-generation sequencing of barcodes the survival and relative fitness of the approximately 150,000 barcoded mutants in the library can be tracked under control as well as experimental conditions. In this way, the *S. elongatus* RB-TnSeq library can be used for pooled, quantitative, whole-genome mutant screens.

In interaction RB-TnSeq (IRB-Seq), the survival of library mutants is observed under a genetic perturbation instead of or in addition to the environmental perturbations normally used in RB-TnSeq. In practice, a second mutation is added to all RB-TnSeq library members; this procedure combines the second mutation with every other individual mutation in the library so that the fitness impact of each double mutant can be determined. In this case, the second mutation inactivated *cdaA* and conferred a different antibiotic resistance than the transposons used to construct the original mutant library (see Materials and Methods). As a control for changes to the library caused by the addition of a second mutation that are not specific to *cdaA* mutation, a non-deleterious mutation was added to a separate aliquot of the initial library. The experimental and control double-mutant libraries were then grown under dual selection so that every member of the library also contained the secondary mutation of interest (*cdaA* or the control). At this point the barcodes of the two double-mutant libraries were sequenced and compared (Fig 3B). These data were used to determine genetic interactions, or instances in which the fitness effects of the library mutation and the *cdaA* mutation are not simply additive (see Materials and Methods). These interactions could in turn be used to identify relationships between genes. In addition, because of the *cdaA* mutant's decreased viability in LDCs, we sensitized our library of double mutants by exposure to LDCs (Fig 3C). Frequencies of the barcodes after this stress were compared to a genotypic and environmental control (see Materials and Methods). In this way IRB-Seq enabled a quantitative assay of genetic interactions with *cdaA*, under both control and sensitizing environmental conditions.

Before attempting IRB-Seq we ensured that the double-mutant library retained sufficient diversity for meaningful functional screens. Of the original 154,949 barcoded mutants in the library, we were able to recover, on average, 100,180 (65%) after addition of the second mutation. This number still represents approximately 30 insertion mutants for the average gene. To further test efficacy of the double-mutant library for screens we used the version containing the control mutation to reproduce the results of a previous screen for LDC-sensitive genes [29]. The screen of the control double-mutant library was conducted under different light conditions than that of the previous single-mutant library screen, and in flasks instead of bioreactors, but nevertheless the two screens strongly correlate ($r = 0.85$; Fig 4A). It is of note that the slope of the regression of the double-mutant screen on the single-mutant screen is approximately 0.4, suggesting that, although the relative phenotypes were similar, the mutants did not diverge as much over the course of the double-mutant experiment. The described changes in the experimental conditions could account for this difference. Based on these results we carried out IRB-Seq using a *cdaA* deletion mutation added to the *S. elongatus* RB-TnSeq library.

IRB-Seq interaction screen. The first genetic interactions examined were those that are detectable under standard laboratory conditions upon the addition of the *cdaA* mutation to the library (Fig 3B). As expected, given that the *cdaA* mutant shows no fitness defects under control conditions (Fig 2A), all of the strong genetic interactions (FDR < 0.01, genetic interaction score absolute value > 1) were negative (aggravating or synthetic interactions) (Fig 4B, S1 Dataset). Such synthetic interactions can result from redundancy in the function associated

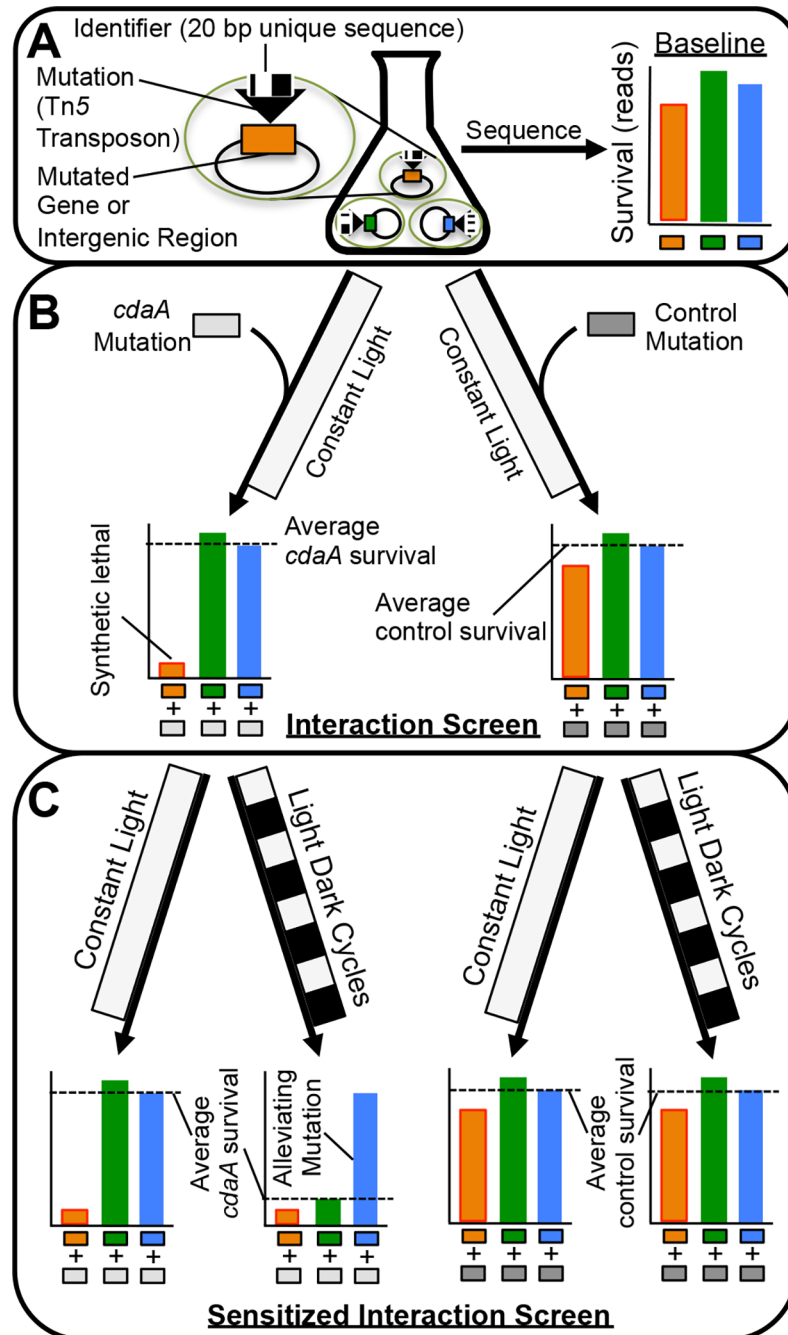


Fig 3. IRB-Seq approach to genetic interaction screens. (A) Each mutant in the starting library contains a loss-of-function mutation with a unique identifier sequence (barcode) that has been previously linked to the mutation's locus. After the archived library is thawed the barcodes present in each mutant are sequenced using next-generation sequencing to determine their baseline levels. (B) The library is then split into two aliquots with one receiving an experimental mutation (AM5403 for this screen), and one receiving a control mutation with no expected fitness costs (AM5329 for this screen). After outgrowth, these two aliquots are sequenced for barcode quantification and compared, which allows identification of genetic interactions between the experimental mutation and the preexisting barcoded mutations. (C) The double mutant library is grown under a condition of stress for the experimental mutation and a four-way comparison between it and controls for genotype and stress condition enables identification of genetic interactions.

<https://doi.org/10.1371/journal.pgen.1007301.g003>

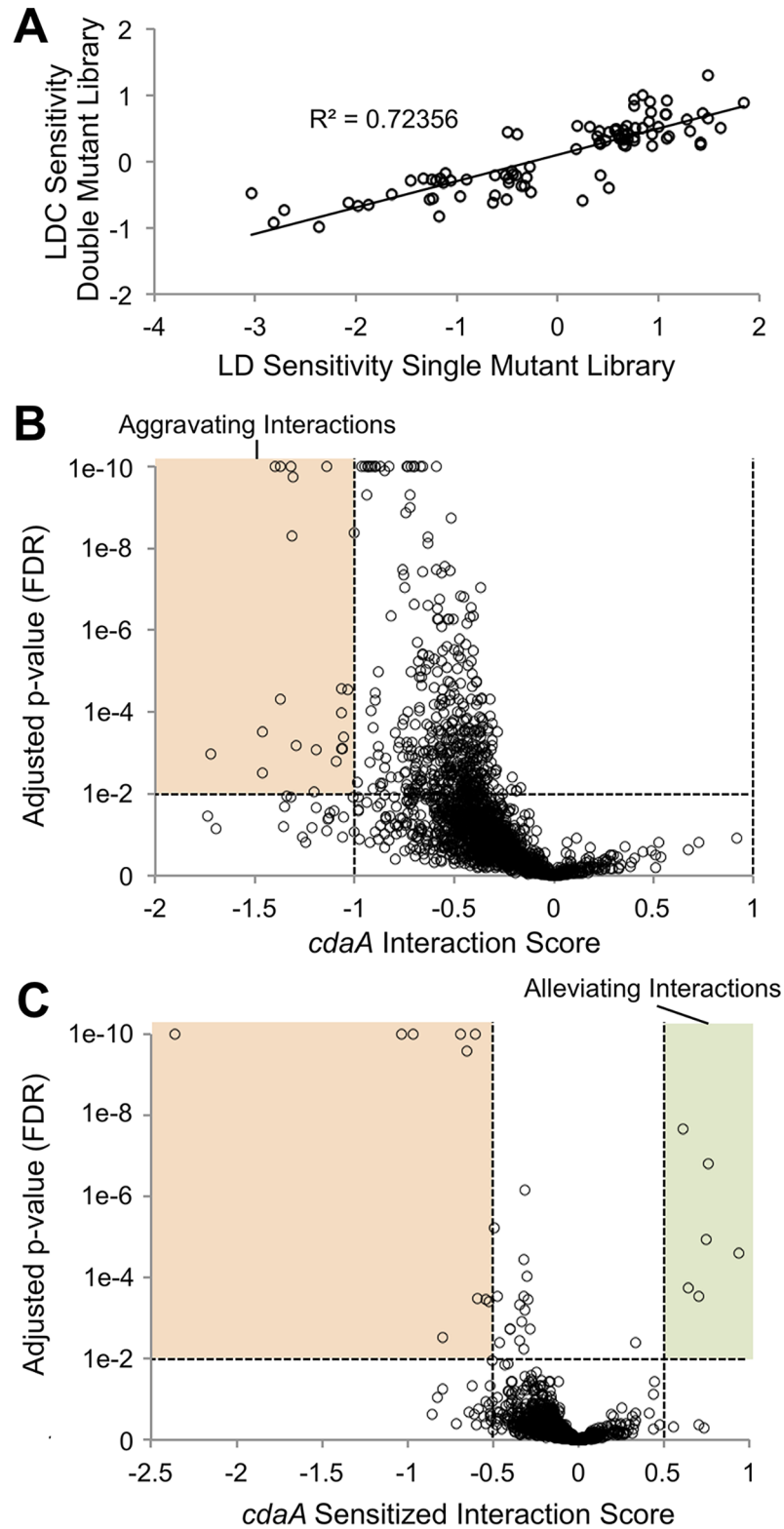


Fig 4. *cdaA* genetic interactions using IRB-Seq. (A) Validation of double-mutant screening by comparison to the previous single-mutant library LDC-sensitivity screen. Each circle represents a gene's score for LDC sensitivity from a previously conducted screen of LDCs on the single-mutant library (x-axis), compared to a similar screen conducted here on a double-mutant library that carries a control mutation (y-axis). A linear regression analysis was used to

determine correlation. (B and C) Plots of (B) genetic interactions and (C) LDC-sensitized genetic interaction of library genes with *cdaA*. Genes above the horizontal dashed line have $FDR < 0.01$ (Linear mixed-effects model). Absolute values of interaction score thresholds of (B) 1 or (C) 0.5 are indicated by vertical dashed lines. All points with $FDR < 10^{-10}$ are plotted as $FDR = 10^{-10}$.

<https://doi.org/10.1371/journal.pgen.1007301.g004>

with the two mutated genes. Two of the top annotated synthetic interactions with *cdaA* were with genes that encode flavoproteins Flv1 (Synpcc7942_1810) and Flv3 (Synpcc7942_1809), which form a heterodimer that allows the release of high-energy electrons from photosystem I to oxygen without producing reactive oxygen species. Although these proteins are dispensable under standard laboratory conditions, they become important for decreasing oxidative stress and allowing growth under variable conditions such as fluctuating light [30,31]. Also in the top ten annotated synthetic interactions were genes that encode a 6-pyruvoyl-tetrahydropterin synthase-like protein potentially involved in a pathway important for resisting UV-A stress (Synpcc7942_1184) [32–34], a glutaredoxin-related protein (Synpcc7942_1145), and Psb28 (Synpcc7942_1679), a protein involved in repair of photosystem II in related cyanobacteria [35]. These interactions suggest that, in the absence of the functional *cdaA*, a cell under increased oxidative stress (Fig 2D) becomes more dependent on proteins that offer electron sinks or protection against reactive oxygen species.

We used targeted loss-of-function mutants to validate the genetic interactions between oxidative stress-related genes and *cdaA* observed through IRB-Seq. A double mutant of *cdaA* and the oxidative stress-related gene with the strongest aggravating interaction, *flv1*, was grown in liquid culture in competition with the *cdaA* single mutant. The double mutant showed drastically decreased survival in comparison with the *cdaA* single mutant (S6A Fig), as expected based on the IRB-Seq results. This effect was much greater than that of the single *flv1* mutant (S6B Fig), suggesting a real aggravating interaction in the double mutant. The results support *cdaA*'s interaction with oxidative stress as well as the ability of IRB-Seq to identify genetic interactions.

Another synthetic interaction apparent from the screen under standard laboratory conditions is with potassium transport. The fifth-ranked aggravating interaction candidate is the K^+ transport protein, TrkH, encoded by *synpcc7942_1080*. Its genomic neighbor, *synpcc7942_1081*, is the second-ranked aggravating interactor. Although Synpcc7942_1081 is unannotated, it is predicted to contain a TrkA domain (PF02080) [36], a complex partner of TrkH [37]. Therefore, the *cdaA* mutant is likely sensitized to defects in potassium import.

Given the genetic interaction with potassium transport, we also tested for physical interaction of c-di-AMP with a potassium transporter. TrkH and Synpcc7942_1081 do not have homologs known to bind c-di-AMP. However, another potassium transport-related polypeptide in *S. elongatus*, KdpD (Synpcc7942_1729), has been found in *S. aureus* to bind c-di-AMP [38,39]. KdpD is a sensor kinase involved in regulation of the Kdp potassium transport system. DRaCALA, a method based upon differential diffusion of bound and unbound radiolabelled c-di-AMP across a nitrocellulose membrane [40], indicates binding of c-di-AMP to *S. elongatus* KdpD (S7 Fig). This finding supports the physiological importance of c-di-AMP in potassium homeostasis in *S. elongatus*.

IRB-Seq sensitized interaction screen. When the *cdaA* double mutant library was sampled under sensitizing LDCs (Fig 3C), we again observed synthetic interactions, but now also observed a number of positive (alleviating interactions) (Fig 4C, S2 Dataset). Alleviating interactions can occur when the affected genes are in the same pathway and their individual and combined effects are equivalent, or when the mutations counteract each other. The presence of synthetic interactions in the sensitized screen can be explained as genes whose loss

exacerbates the moderate survival impact of the *cdaA* mutation in LDCs. For the sensitized interaction screen, we decreased the interaction score for consideration to greater than absolute value of 0.5. This change was based on our observation that the selection strength of the LDC screening conditions enabled the differentiation of genuine, but subtle, mutant phenotypes (Fig 4A). Among the six alleviating candidates for *cdaA* in LDCs (FDR < 0.01, genetic interaction > 0.5) four are proteins involved in macromolecule degradation. The cell wall recycling protein MurQ (Synpcc7942_2577), the top hit among alleviating interactions, may be explained by decreased cell wall turnover being permissive in the *cdaA* mutant, which has been associated with disruption of cell wall homeostasis in multiple species [2]. The reason for the more general enrichment of genes that encode degrading enzymes among alleviating mutations is unclear.

The fifth-ranked hit among suppressors and the strongest hit among the synthetic interactions were circadian clock component CikA (Synpcc7942_0644) and circadian-involved sigma factor RpoD2 (Synpcc7942_1746), respectively. Mutants of *cikA*, the phosphatase for the master clock transcription factor RpaA, leave RpaA in a highly phosphorylated state [41]. This RpaA state locks the clock into activating nighttime processes and the detoxification of oxidative stress [27,42,43]. The single *cikA* mutant has a slightly positive effect on light-dark survival and has been shown to be capable of alleviating another LDC-sensitive mutant, *kaiA* [29]. Therefore, it might be expected that the *cdaA* mutant, which is unable to fully clear oxidative stress and survive the night, would be suppressed by *cikA*. The *rpoD2* gene, which has by far the strongest synthetic interaction with *cdaA* in the sensitized screen, encodes a sigma factor that causes changes in circadian rhythms when mutated [44]. However, the broader transcriptional and physiological effects of this mutation are unknown, and when the interaction was tested with targeted loss-of-function mutations, it was not supported (S8 Fig). It is unclear whether this result is due to a technical shortcoming in the follow-up experiment, a difference in the behavior of the *rpoD2-cdaA* double mutant in the mixed library population and in a two-member competition, or an inaccurate sensitized interaction call by IRB-Seq. Therefore, the presence and nature of an interaction of *cdaA* with the circadian clock is yet uncertain.

Discussion

These investigations present the use of classical molecular biology and the newly developed IRB-Seq approach to characterize *c*-di-AMP in the model cyanobacterium, *S. elongatus*. The molecule exists in *S. elongatus* at concentrations that are likely physiologically relevant. It is synthesized by the product of the previously unannotated gene *synpcc7942_0263* (assigned here as *cdaA*). One important physiological function of CdaA appears to be survival through LDCs, which is impaired in the *cdaA* mutant (Fig 2). This finding suggests a role for *c*-di-AMP as an intracellular signal of LDCs. Finally, through the use of IRB-Seq, we determined the interaction landscape of *c*-di-AMP, which links the signaling nucleotide to oxidative stress management and potassium transport. This work expands our understanding of the intracellular signaling mechanisms in *S. elongatus*, illuminates new roles of *c*-di-AMP, and describes a high-throughput approach for identifying genetic interactions.

The non-essential nature of *c*-di-AMP in *S. elongatus*

C-di-AMP controls many aspects of bacterial physiology and is essential in the bacterial phylum Firmicutes, where most research on the molecule has taken place. The essential nature of *c*-di-AMP has been connected to its role in central metabolism [45], its linkage to levels of another signaling nucleotide (p)ppGpp [11], and its role in potassium homeostasis [46]. Importantly, the absence of *c*-di-AMP is lethal in Firmicutes in rich media, whereas minimal

media are permissive for a null mutant. A possible explanation for *S. elongatus*' viability with the *cdaA* mutation is that, as a photoautotroph, it is far more independent of nutrients in the medium than the previously studied heterotrophs. Regardless of its cause, the essential nature of c-di-AMP in many organisms has limited the ability to study this nucleotide [21]. Future genetic exploration of *cdaA* will be facilitated by the viability of the *S. elongatus cdaA* mutant.

The IRB-Seq approach to genetic interaction screens

The IRB-Seq approach developed for this study enables high-throughput quantitative genetic interaction screens with minimal sequencing prep. In the approach, a second mutation is added directly to an existing RB-TnSeq library, removing the need of previous approaches to recreate a library in a new background and re-determine all insertion loci for each screen (Fig 3) [13–15]. Traditional sequencing preparation used in classical Tn-Seq studies is also avoided because survival of mutants is quantified by PCR and sequencing of 20 bp “barcodes” present in each transposon which serve as identifiers for each clone in the mutant library (BarSeq) [18]. IRB-Seq requires only one PCR and $\sim 1/100^{\text{th}}$ of an Illumina HiSeq 4000 lane per sample to provide a genome-wide quantitative measure of genetic interactions ranging from strong alleviation to full synthetic lethal. The advantage of a quantitative alternative to previous suppressor screens used in c-di-AMP research [11,12] is particularly apparent in this study. The *cdaA* mutant's lack of fitness phenotype under constant light, and moderate phenotype under sensitizing LDCs, would have made traditional suppressor screens difficult, and likely ineffective. In addition, the high-throughput nature of this approach to genome-wide genetic interaction screens makes it feasible to conduct IRB-Seq screens in replicate and under many different sensitizing and permissive conditions.

Potential causes of c-di-AMP spike at night

While this work does not determine the mechanism of the CdaA mediated c-di-AMP increase after darkness, several possibilities can be considered in light of the literature. One potential explanation is a transcriptional increase around dusk of c-di-AMP's cyclase, CdaA, potentially controlled by the circadian clock. However, the immediate change in c-di-AMP level upon onset of darkness (Fig 1D), combined with a lack of dusk- or dark-induced expression of *cdaA* [47–49], make circadian or transcriptional control unlikely. Nor does the quantity of CdaA's substrate, ATP, increase in darkness [50,51], and thus is not likely to explain the increases in c-di-AMP. Therefore, it is more likely that the spike in c-di-AMP level results from dark-dependent changes in the activity of CdaA or c-di-AMP's phosphodiesterase.

Illuminating the role of c-di-AMP in nighttime survival

Elucidating the survival of Cyanobacteria in LDCs is important for improved understanding of both a phylum of tremendous ecological importance and an environmental challenge relevant to all photosynthetic organisms. For ease of research, however, most experiments on cyanobacteria have been conducted in simplifying constant-light conditions. The work in LDCs that exists shows oxidative stress management as a key component for surviving LDCs [27,29]. Similarly to the LDC-sensitive circadian clock mutants of *rpaA* and *kaiA*, lethality in the *cdaA* mutant occurred specifically upon the onset of night following high oxidative stress at dusk (Fig 2). The death in the mutant begins concurrent with a spike in c-di-AMP level in the WT (Fig 1D). This correlation suggests a role for the molecule in the day-night transition, a seemingly crucial period for surviving LDCs in the mutants where it has been studied. This role is further supported by the finding that a number of the top *cdaA* synthetically interacting genes determined by IRB-Seq are involved in oxidative stress mitigation. Thus, c-di-AMP appears to

be involved in LDC survival through management of oxidative stress, a characteristic shared with LDC-sensitive clock mutants.

A possible basis for the *cdaA* mutant's sensitivity to LDCs and oxidative stress may be potassium transport. C-di-AMP has previously been associated with multiple potassium transporters [2]. In *S. aureus* c-di-AMP negatively regulates the Kdp potassium uptake system through its binding to the histidine kinase KdpD [38]. In this study KdpD was suggested by DRaCALA to bind c-di-AMP in *S. elongatus*. Additionally, two proteins from the Trk family of potassium transporters (Synpcc7942_1080 and Synpcc7942_1081) were found among the top synthetic interactions, suggesting that the *cdaA* mutant is sensitized to potassium transport mutations. Altered potassium transport previously has been shown in cyanobacteria to sensitize the cells to the oxidative stress-producing conditions of high light and heavy metal exposure [52,53]. Therefore, the canonical role of c-di-AMP in potassium homeostasis may, in *S. elongatus*, be involved in the non-canonical function of LDC survival through oxidative stress regulation.

Future uses of IRB-Seq

IRB-Seq is an inexpensive and straightforward approach to high-throughput quantitative interaction screens and is suitable for addressing an array of questions in different organisms. With 25 published RB-TnSeq libraries [28,54] and many more under development, there exists ample starting material for IRB-Seq screens, assuming the ability to deliver a second mutation into the host with high efficiency. In this case, natural transformation was sufficient to generate the double-mutant library, but other techniques such as conjugation may be necessary for species that are not naturally competent. The experimental pipeline and analysis tools developed here make this assay feasible for genetic interactions of any gene of interest. Furthermore, the addition of multiple mutations into the library, or reporters paired with cell sorting, should enable screening for more complex genetic interactions as well as identification of effects on gene expression by genetic perturbations.

Materials and methods

Strains and culture conditions

WT in this study and the background for all mutants was *Synechococcus elongatus* PCC 7942, stored in our lab as AMC06. For all experiments, growth was conducted in BG-11 media with appropriate antibiotics at 30°C [55]. Unless otherwise indicated, liquid culture growth was under constant light in 250 mL flasks containing 100 mL of culture shaken at 150 rpm (Thermo Fisher MaxQ 2000 Orbital Shaker).

Targeted mutants

For mutagenesis by transformation, standard *S. elongatus* protocols [55] were altered for dark-sensitive mutants. The typical overnight incubation in darkness after DNA addition was instead performed under 70 $\mu\text{mol photons}\cdot\text{m}^{-2}\cdot\text{s}^{-1}$. For experiments using *cdaA* loss-of-function mutants, with the exclusion of IRB-Seq and IRB-Seq validation experiments, the plasmid for insertion mutagenesis (8S16-L9, conferring kanamycin (Km) resistance) was from the previously published unigene set [56]. For IRB-Seq and IRB-Seq validation experiments, which required a loss-of-function strain with an antibiotic resistance other than Km, a *cdaA*-deletion plasmid (AM5403) carrying the spectinomycin- (Sp) and streptomycin- (Sm) resistance gene *aadA* was constructed using CYANO-VECTOR procedures and devices [57]. This deletion

removed a region from 8 bp upstream to 575 bp downstream of the translation start site of *cdaA*.

cdaA LDC characterization

Phenometrics ePBR photobioreactors (version 1.1; Phenometrics Inc.) were used in LDC liquid culture assays for measurement of: survival, OD₇₅₀, c-di-AMP quantity, and ROS. The bioreactors were inoculated with 400 mL of culture at OD₇₅₀ = 0.1. They were then grown under 150 μmol photons·m⁻²·s⁻¹ with filtered air bubbled in at a rate of 50 mL/min. After 12 h, the bioreactor cultures were re-diluted to OD₇₅₀ = 0.1 and exposed to a 12:12 h LDC for purposes of low-light entrainment of the circadian clock; dark-sensitive mutants were previously shown to survive at this light intensity in the bioreactors [27]. After this entrainment cycle the light intensity was increased to the restrictive condition of 500 μmol photons·m⁻²·s⁻¹ for the remaining LDCs, at which point assays for physiology were conducted.

High-resolution measurement of survival, c-di-AMP quantity, ROS, and absorbance spectrum were all conducted immediately following the increase of the bioreactors' LDC light intensity to 500 μmol photons·m⁻²·s⁻¹. Survival was measured using a 1:5 dilution series over 8 wells with the first well containing a 1:10 dilution of the bioreactor culture. The 8 dilutions were plated in 4 μL spots on solid medium and incubated under continuous illumination at 150 μmol photons·m⁻²·s⁻¹ for 5 d, at which point they were photographed. The photographs were then analyzed for colony forming units (CFUs) and for surface area of the colonies using ImageJ [58]. For quantification of c-di-AMP, 1.5 mL of culture was sampled, pelleted at 4 C at 20,000 g for 3 min, and resuspended in 500 μL methanol with 20 μL of 0.5 μM heavy-labeled c-di-AMP. The mixture was then stored at -20 C until quantification (See C-di-AMP quantification). ROS was quantified on 1 mL of culture using the fluorescent marker H₂DCFDA (Life Technologies catalog no. D399) as described previously [27]. Absorbance spectra were taken using a Tecan Infinite M200 plate reader.

LDC-specific sensitivity assays were also conducted on plates. A 1:5 dilution series over 8 wells was made for *cdaA* and a WT with the first well containing culture at OD₇₅₀ = 0.02. These dilutions of *cdaA* and a WT were then plated in 4 μL spots on duplicate plates. One of these plates was grown under 125 μmol photons·m⁻²·s⁻¹ constant light for 5 d, while the other was grown under 125 μmol photons·m⁻²·s⁻¹ LDCs for 8 d. Although LDCs at this light intensity are permissive in the bioreactors, they constitute a restrictive condition for dark-sensitive mutants on plates, where there is no self-shading by the culture.

C-di-AMP biochemical and proteomic quantification

C-di-AMP quantification. Samples stored at -20°C for c-di-AMP quantification (from: *cdaA* LDC Characterization) were pelleted, resuspended in 50 μL of 0.5 μM heavy-labeled c-di-AMP, and then mixed with 500 μL of methanol and sonicated. After centrifugation of lysed cells, the supernatant fraction was collected. The remaining pellet was resuspended in 50 μL of H₂O, mixed with 500 μL of methanol, and centrifuged again to collect a second supernatant fraction. Both methanol fractions were pooled and evaporated, and the final pellet containing c-di-AMP was resuspended in 50 μL of double distilled H₂O. Mass spectrometry analysis was performed as previously described [9]. Intracellular concentrations of c-di-AMP were determined using the cell volume of 2.47 e⁻¹⁰ L, which was estimated using length 2.512 μm and width 1.118 μm [59].

C-di-AMP binding assay. Binding validation was conducted with radiolabeled c-di-AMP using the DRaCALA approach as previously described [9]. Protein candidates identified as interacting with c-di-AMP sepharose beads were expressed from pET20b and pMAL vectors

in *Escherichia coli* BL21. Following induction, *E. coli* cell lysates were incubated with radiolabeled c-di-AMP, spotted on nitrocellulose membrane, and visualized with a Typhoon imager (GE Healthcare).

IRB-Seq

Interaction screen. To look for genetic interactions of *cdaA* with the mutated loci in the previously created RB-TnSeq library [28], the library was transformed with a *cdaA* deletion mutation plasmid (AM5403) and separately a Neutral Site I control mutation plasmid (AM5329). An aliquot of the *S. elongatus* RB-TnSeq library was first thawed as previously described [28]. Before transformation, 4 T_0 samples were taken with the equivalent of 10 mL at $OD_{750} = 0.3$, and were pelleted and frozen at -80°C . Transformation was conducted in triplicate with the *cdaA* deletion vector and the control vector (6 transformations total) using the modified transformation protocols described above in which no dark incubation was included. Both plasmids contained Sp and Sm resistance cassettes to allow selection in the Km resistant background of the RB-TnSeq library. To maintain the diversity of the $1.52 \cdot 10^5$ -member library, we attempted to plate a total of approximately $5 \cdot 10^5$ mutants over 10 plates for each replicate of $\Delta cdaA$ ($4.38 \cdot 10^5$ average/replicate mutants achieved) and control ($5.31 \cdot 10^5$ average/replicate mutants achieved) double-mutant libraries (60 plates total). After growth for 4 d in $140 \mu\text{mol photons} \cdot \text{m}^{-2} \cdot \text{s}^{-1}$ under Km, Sp, and Sm selection, plates were harvested and combined into 6 tubes (one for each replicate and experimental condition). At this point two samples for each tube, equivalent to 10 mL at $OD_{750} = 0.3$, were pelleted and frozen at -80°C . These samples served as both the post-selection samples for the interaction screen and the T_0 samples for the sensitized interaction screen. Because direct transformation was used to introduce the *cdaA* deletion and control mutation, any barcoded mutants that disable transformation were not represented in the resulting double-mutant libraries.

Sensitized interaction screen. The tubes containing the harvested interaction screen plates were used as inocula for the LDC-sensitized interaction screen. Flasks containing 100 ml BG-11 for each replicate and genotype were inoculated in duplicate at $OD_{750} = 0.01$ (12 flasks total). The duplicates were then split into constant light and 12:12 h LDCs. Both light conditions were conducted under $30 \mu\text{mol photons} \cdot \text{m}^{-2} \cdot \text{s}^{-1}$ for the first 24 h period as entrainment for the LDC flasks, after which light intensity was increased to $150 \mu\text{mol photons} \cdot \text{m}^{-2} \cdot \text{s}^{-1}$ for all flasks, a condition determined to be restrictive for dark-sensitive mutants. Once the cultures had grown to approximate OD_{750} of 0.64 (6 generations), two 5 mL samples for each were pelleted and frozen at -80°C . These samples would be compared to the T_0 samples taken after the double-mutant library was harvested from plates (See Interaction screen). All samples from the interaction screens had genomic DNA extracted [55], and survival of constituent mutants quantified, using the previously developed BarSeq protocol [18].

Interaction screen analysis. To estimate genetic interactions, the survival of library constituents containing the *cdaA* mutation were compared to those containing the control mutation. A similar analysis had been conducted previously with the untransformed library to identify differential survival of the single mutants in the presence and absence of LDCs [29]. The current analysis was conducted identically, except we considered the $\Delta cdaA$ background of the library to be the experimental condition and the control mutation background to be the control condition. As in Welkie et al. [29], we removed 24,868 barcodes falling outside of annotated genes and 27,763 barcodes that were not within the middle 80% of genes. We also removed any gene represented by fewer than three barcodes in different positions. This curation resulted in 102,136 barcodes distributed across 1,961 genes remaining for further analysis.

To avoid errors when log-transforming the read counts, we added a pseudocount of one to the number of reads for a barcode for each sample. We then divided this value by the total number of reads in the sample calculated before any pruning, and log-2 transformed this sample-normalized number of reads.

In the experiment a single starting pool (T_0) of barcoded strains was split into 3 control and 3 experimental samples. The log-2 count for a barcode from the starting pool was subtracted from the values for the 6 derived samples. We then discarded any gene without at least 15 reads in the starting pool and summed across barcodes before adding the pseudocount (41/1961), leaving 1920 genes and 101,876 barcodes.

To determine an interaction score for each gene, we used R [60] to fit a pair of nested linear mixed effects models to the sample- and read-normalized log-2 transformed counts using maximum likelihood (S3 Dataset):

$$y_{i,j,k} = \mu_g + T_j + B_i + \varepsilon_{i,j,k}; B_i \sim iid N(0, \varsigma_g^2); \varepsilon_{i,j,k} \sim iid N(0, \sigma_g^2) \quad (1)$$

$$y_{i,j,k} = \mu_g + B_i + \varepsilon_{i,j,k}; B_i \sim iid N(0, \varsigma_g^2); \varepsilon_{i,j,k} \sim iid N(0, \sigma_g^2) \quad (2)$$

where $y_{i,j,k}$ is the normalized log-2 value for barcode i in gene g with genetic background j for sample k , μ_g is the average value for the gene, T_j is the fixed effect of genetic background j , B_i is a random effect for barcode i , and $\varepsilon_{i,j,k}$ is the residual. We identified genes with significant fitness differences between genetic backgrounds by comparing the difference in the -2^* log likelihoods of the models to a chi-square distribution with one degree of freedom, estimating a p-value, and accounting for multiple testing by controlling the false discovery rate [61]. We selected those genes with adjusted p-values less than 0.01. We took the contrast $T_{\Delta cdaA} - T_{wt}$ to be the estimated fitness effect of knocking out the gene between the genetic backgrounds.

Sensitized interaction screen analysis. The sensitized-interaction screen involved six different starting pools (T_0) of barcoded strains (3 with the control vector genetic background, 3 with a $\Delta cdaA$ genetic background). Each T_0 pool was divided into constant light and LDC samples. We proceeded as above through log-2 transforming the sample-normalized number of reads. To account for different starting percentages of each barcode within the T_0 pools, we subtracted the starting barcode values from the values after constant light or LDC growth for each sample. We also removed the 232 genes represented by fewer than 15 T_0 reads in each pool, leaving 1,729 genes and 98,216 barcodes.

To determine a sensitized-interaction score for each gene, we used maximum likelihood to fit a pair of nested linear mixed effects models to the sample- and read-normalized log-2 transformed counts (S4 Dataset):

$$y_{i,j,k,m} = \mu_g + C_j + T_m + (C_j * T_m) + B_i + \varepsilon_{i,j,k,m}; B_i \sim iid N(0, \varsigma_g^2); \varepsilon_{i,j,k,m} \sim iid N(0, \sigma_g^2) \quad (3)$$

$$y_{i,j,k,m} = \mu_g + C_j + T_m + B_i + \varepsilon_{i,j,k,m}; B_i \sim iid N(0, \varsigma_g^2); \varepsilon_{i,j,k,m} \sim iid N(0, \sigma_g^2) \quad (4)$$

where $y_{i,j,k,m}$ is the normalized log-2 value for barcode i in gene g in condition j for sample k in genetic background m . μ_g is the average value for the gene; C_j is the fixed effect of condition j (either constant light or LDCs); T_m is a fixed effect of the genetic background (either wt or $\Delta cdaA$); B_i is a random effect for barcode i ; and $\varepsilon_{i,j,k,m}$ is the residual. ($C_j * T_m$) represents the interaction between light condition and genetic background and estimates the effect in which we are interested—whether fitness difference for a strain between constant light and LDC conditions depends on the genetic background. By determining how well model (3), which includes the interaction term, fits the data compared to model (4), which does not, we can test whether the genetic background significantly affects the fitness difference. We identified genes

for which model (3) fit significantly better than model (4) by comparing the difference in the $-2 \cdot \log$ likelihoods of the models to a chi-square distribution with one degree of freedom, estimating a p-value, and accounting for multiple testing as above by adjusting our p-values and accepting a false discovery rate of 0.01. We took the contrast $(C_{LD}T_{\Delta cdaA} - C_{LD}T_{wt}) - (C_{LL}T_{\Delta cdaA} - C_{LL}T_{wt})$ to estimate the fitness effects of the interaction between light condition and genetic background.

Competition assays for validation of IRB-Seq

For one-on-one competition experiments single mutants were prepared for *cdaA* (AM5403) with Sp and Sm resistance, the putatively interacting mutants of interest carrying Km resistance, and WT controls for both Km resistance (8S15-K12), and Sp and Sm resistance (AM1303). Double mutants with the *cdaA* loss-of-function background and the putatively interacting second mutation were also prepared. The mutants were grown to $OD_{750} \sim 0.4$ and washed three times with BG-11 without antibiotics via centrifugation at 4,696 G for ten minutes and diluted to an OD of 0.015. Cultures were then mixed in a 1:1 ratio according to the desired competition being assayed and grown for 8 days under $\sim 100 \mu\text{mol photons}\cdot\text{m}^{-2}\cdot\text{s}^{-1}$.

Composition of competing populations was determined by leveraging the different antibiotic resistances of the strains. To assay survival of each genotype at zero, three, and eight days, mixed culture was serially diluted using a 1:10 dilution series over 6 wells. The dilutions were plated in 20 μL spots in duplicate onto $\sim 2 \text{ mL}$ of BG-11 agar with either Sp and Sm, or Km on a 24-well clear plate. Colony number from the dilution series across the two antibiotic regimes was used to calculate CFUs in the original competition culture. Differentiation of the CFUs for the double mutants (Km-, Sp and Sm-resistant) and single *cdaA* mutants (Sp- and Sm-resistant) was accomplished via subtraction of the CFUs growing on Km from those growing on Sp and Sm.

Supporting information

S1 Fig. Genotyping of the *cdaA* insertion mutant. On the left, the location of the transposon insertion mutation conferring Km resistance is shown over a schematic drawn to scale of the gene. On the right, the genotyping gel containing lanes: 1, amplification of *cdaA* mutant allele (8S16-L9), in which a 1.3 kb insertion is present, with primers surrounding the *cdaA* gene; 2, amplification of WT DNA with the same primers; 3, standard 1-kb ladder (New England Bio-Labs).
(PDF)

S2 Fig. Mass spectrometry chromatograms of WT and *cdaA* mutant extracts. Each sample was mixed with an internal standard (heavy labeled c-di-AMP), detected as m/z 689 \rightarrow 146 transition. Biological c-di-AMP was detected through four m/z transitions: 659 \rightarrow 136 (as a qualifier and quantifier), 659 \rightarrow 312 (as a qualifier), 659 \rightarrow 330 (as a qualifier). (A) In WT extracts, all transitions corresponded well with the internal standard; (B) whereas in *cdaA* mutant extracts, only noise was detected.
(PDF)

S3 Fig. Expression of *S. elongatus cdaA* in *E. coli*. The *S. elongatus cdaA* gene was expressed in a modified version of the IPTG inducible vector pMAL-c2X in DH5 α (AM5466). Fold change is shown relative to uninduced vector. Error bars represent SE of two replicates.
(PDF)

S4 Fig. Complementation of the *cdaA* mutant. The top panel shows the phenotype, measured by spot plate, of the *cdaA* mutant (8S16-L9) under constant light and LDCs. The bottom

panel shows the phenotype of the *cdaA* mutant when a WT allele of the *cdaA* gene is added in trans to neutral site two (using vector AM5253). *** $P < 10^{-3}$.
(PDF)

S5 Fig. Absorbance spectrum of *cdaA* mutant during a LDC. Mean absorbance values of the *cdaA* transposon mutant (8S16-L9) and WT at (A) 0 h, (B) 30 h, and (C) 36 h into an LDC. Absorbance is normalized to OD₇₅₀ and each value represents the average of four replicates.
(PDF)

S6 Fig. Genetic interaction with *flv1*. (A) Relative survival of the *cdaA* single mutant and the *cdaA-flv1* double mutant when grown competitively against each other. (B) Relative survival of WT and the *flv1* single mutant when grown competitively against each other. In all figure parts survival is determined by spot plates (see [Materials and Methods](#)) and error bars represent SE of three replicates.
(PDF)

S7 Fig. Binding of c-di-AMP by KdpD. Binding of KdpD (Synpcc7942_1729) expressed in *E. coli* to c-di-AMP, determined by DRaCALA on cell lysate (see [Materials and Methods](#)). Error bars indicate SE of two replicates.
(PDF)

S8 Fig. Assaying *rpoD2* for sensitized genetic interaction. (A) Relative survival of the *cdaA* single mutant and the *cdaA-rpoD2* double mutant when grown competitively against each other in constant light and LDCs. (B) Relative survival of WT and the *rpoD2* single mutant when grown competitively against each other in constant light and LDCs. Survival in all figure parts is determined by spot plates (see [Materials and Methods](#)) and error bars represent SE of three replicates.
(PDF)

S1 Dataset. *cdaA* mutant genetic interactions.
(XLSX)

S2 Dataset. *cdaA* mutant sensitized genetic interactions.
(XLSX)

S3 Dataset. Interaction screen R script. This file contains the annotated R script for determining genetic interactions, where two genetic backgrounds within the library are compared. Also included are the files on which the script was run to produce interaction scores for the *cdaA* mutant: 1) “all.poolcount.txt”, the location and reads of barcoded transposon mutants for each sample; 2) “interaction_screen_exp.csv”, with designation of the samples as T₀, control genotype, and experimental genotype; 3) “genes.tab”, the gene coordinate file used to map barcoded transposon mutants to genes.
(ZIP)

S4 Dataset. Sensitized interaction screen R script. This file contains the annotated R script for determining sensitized genetic interactions, where two genetic backgrounds within the library are compared under two environmental conditions. Also included are the files on which the script was run to produce sensitized interaction scores for the *cdaA* mutant: 1) “Interaction_LD_all_pool.csv”, the location and reads of barcoded transposon mutants for each sample under LDCs; 2) “Interaction_LL_all_pool.csv”, the location and reads of barcoded transposon mutants for each sample under constant light; 3) “interaction_screen_exp.csv”, with designation of sample light regime, group (whether the samples are from the same or different T₀s), and whether they are T₀, control genotype, or experimental genotype; 4) “genes.”

tab”, the gene coordinate file used to map barcoded transposon mutants to genes. (ZIP)

Acknowledgments

We thank E. Orsi and J. Tan for technical assistance.

Author Contributions

Conceptualization: Benjamin E. Rubin, Spencer Diamond, Ryan Simkovsky, Joshua J. Woodward, Susan S. Golden.

Data curation: Benjamin E. Rubin, Spencer Diamond, Scott A. Rifkin, Susan S. Golden.

Formal analysis: Benjamin E. Rubin, Scott A. Rifkin.

Funding acquisition: Spencer Diamond, Joshua J. Woodward, Susan S. Golden.

Investigation: Benjamin E. Rubin, TuAnh Ngoc Huynh, David G. Welkie, Emily C. Pierce, Laura C. Lowe, Jenny J. Lee, Joshua J. Woodward.

Methodology: Benjamin E. Rubin, Arnaud Taton.

Project administration: Benjamin E. Rubin, Susan S. Golden.

Resources: Arnaud Taton, Joshua J. Woodward.

Software: Ryan Simkovsky.

Supervision: Ryan Simkovsky, Joshua J. Woodward, Susan S. Golden.

Validation: Benjamin E. Rubin, TuAnh Ngoc Huynh, David G. Welkie, Laura C. Lowe, Jenny J. Lee, Joshua J. Woodward.

Visualization: Benjamin E. Rubin, TuAnh Ngoc Huynh, Ryan Simkovsky, Joshua J. Woodward.

Writing – original draft: Benjamin E. Rubin, TuAnh Ngoc Huynh, Joshua J. Woodward.

Writing – review & editing: Benjamin E. Rubin, TuAnh Ngoc Huynh, David G. Welkie, Spencer Diamond, Ryan Simkovsky, Arnaud Taton, Scott A. Rifkin, Joshua J. Woodward, Susan S. Golden.

References

1. Witte G, Hartung S, Büttner K, Hopfner K-P. Structural biochemistry of a bacterial checkpoint protein reveals diadenylate cyclase activity regulated by DNA recombination intermediates. *Mol Cell*. 2008; 30: 167–178. <https://doi.org/10.1016/j.molcel.2008.02.020> PMID: 18439896
2. Corrigan RM, Gründling A. Cyclic di-AMP: another second messenger enters the fray. *Nat Rev Microbiol*. 2013; 11: 513–524. <https://doi.org/10.1038/nrmicro3069> PMID: 23812326
3. Commichau FM, Dickmanns A, Gundlach J, Ficner R, Stülke J. A jack of all trades: the multiple roles of the unique essential second messenger cyclic di-AMP. *Mol Microbiol*. 2015; 97: 189–204. <https://doi.org/10.1111/mmi.13026> PMID: 25869574
4. Flombaum P, Gallegos JL. Present and future global distributions of the marine Cyanobacteria *Prochlorococcus* and *Synechococcus*. *Proc Natl Acad Sci U S A*. 2013; 110: 9824–9829. <https://doi.org/10.1073/pnas.1307701110> PMID: 23703908
5. Bryant DA. The beauty in small things revealed. *Proc Natl Acad Sci U S A*. 2003; 100: 9647–9649. <https://doi.org/10.1073/pnas.1834558100> PMID: 12917493
6. Angermayr SA, Rovira AG, Hellingwerf KJ. Metabolic engineering of cyanobacteria for the synthesis of commodity products. *Trends Biotechnol*. 2015; 33: 352–361. <https://doi.org/10.1016/j.tibtech.2015.03.009> PMID: 25908503

7. Nelson JW, Sudarsan N, Furukawa K, Weinberg Z, Wang JX, Breaker RR. Riboswitches in eubacteria sense the second messenger c-di-AMP. *Nat Chem Biol.* 2013; 9: 834–839. <https://doi.org/10.1038/nchembio.1363> PMID: 24141192
8. Agostoni M, Montgomery B. Survival strategies in the aquatic and terrestrial world: the impact of second messengers on cyanobacterial processes. *Life.* 2014; 4: 745–769. <https://doi.org/10.3390/life4040745> PMID: 25411927
9. Huynh TN, Luo S, Pensinger D, Sauer J- D, Tong L, Woodward JJ. An HD-domain phosphodiesterase mediates cooperative hydrolysis of c-di-AMP to affect bacterial growth and virulence. *Proc Natl Acad Sci U S A.* 2015; 112: E747–56. <https://doi.org/10.1073/pnas.1416485112> PMID: 25583510
10. Hood RD, Higgins SA, Flamholz A, Nichols RJ, Savage DF. The stringent response regulates adaptation to darkness in the cyanobacterium *Synechococcus elongatus*. *Proc Natl Acad Sci U S A.* 2016; 113: E4867–76. <https://doi.org/10.1073/pnas.1524915113> PMID: 27486247
11. Whiteley AT, Pollock AJ, Portnoy DA. The PAMP c-di-AMP is essential for *Listeria monocytogenes* growth in rich but not minimal media due to a toxic increase in (p)ppGpp. *Cell Host Microbe.* 2015; 17: 788–798. <https://doi.org/10.1016/j.chom.2015.05.006> PMID: 26028365
12. Corrigan RM, Abbott JC, Burhenne H, Kaefer V, Gründling A. c-di-AMP is a new second messenger in *Staphylococcus aureus* with a role in controlling cell size and envelope stress. *PLoS Pathog.* 2011; 7: e1002217. <https://doi.org/10.1371/journal.ppat.1002217> PMID: 21909268
13. van Opijnen T, van Opijnen T, Bodi KL, Bodi KL, Camilli A, Camilli A. Tn-seq: high-throughput parallel sequencing for fitness and genetic interaction studies in microorganisms. *Nat Methods.* 2009; 6: 767–772. <https://doi.org/10.1038/nmeth.1377> PMID: 19767758
14. Meeske AJ, Sham L-T, Kimsey H, Koo B-M, Gross CA, Bernhardt TG, et al. MurJ and a novel lipid II flipase are required for cell wall biogenesis in *Bacillus subtilis*. *Proc Natl Acad Sci U S A.* 2015; 112: 6437–6442. <https://doi.org/10.1073/pnas.1504967112> PMID: 25918422
15. Dejesus MA, Nambi S, Smith CM, Baker RE, Sasseti CM, Iroger TR. Statistical analysis of genetic interactions in Tn-Seq data. *Nucleic Acids Res.* 2017; 1–11.
16. Brochado AR, Typas A. High-throughput approaches to understanding gene function and mapping network architecture in bacteria. *Curr Opin Microbiol.* 2013; 16.
17. Gray AN, Koo B-M, Shiver AL, Peters JM, Osadnik H, Gross CA. High-throughput bacterial functional genomics in the sequencing era. *Curr Opin Microbiol.* 2015; 27: 86–95. <https://doi.org/10.1016/j.mib.2015.07.012> PMID: 26336012
18. Wetmore KM, Price MN, Waters RJ, Lamson JS, He J, Hoover CA, et al. Rapid quantification of mutant fitness in diverse bacteria by sequencing randomly bar-coded transposons. *MBio.* 2015; 6: e00306–15–15.
19. Huynh TN, Woodward JJ. ScienceDirect Too much of a good thing: regulated depletion of c-di-AMP in the bacterial cytoplasm. *Curr Opin Microbiol.* 2016; 30: 22–29. <https://doi.org/10.1016/j.mib.2015.12.007> PMID: 26773214
20. Johnson LS, Eddy SR, Portugaly E. Hidden Markov model speed heuristic and iterative HMM search procedure. *BMC Bioinformatics.* 2010; 11: 431. <https://doi.org/10.1186/1471-2105-11-431> PMID: 20718988
21. Xayarath B, Freitag NE. Uncovering the nonessential nature of an essential second messenger. *Cell Host Microbe.* 2015; 17: 731–732. <https://doi.org/10.1016/j.chom.2015.05.015> PMID: 26067599
22. Klotz A, Georg J, Bučinská L, Watanabe S, Reimann V, Januszewski W, et al. Awakening of a dormant cyanobacterium from nitrogen chlorosis reveals a genetically determined program. *Curr Biol.* 2016; 26: 2862–2872. <https://doi.org/10.1016/j.cub.2016.08.054> PMID: 27720620
23. Rosenberg J, Dickmanns A, Neumann P, Gunka K, Arens J, Kaefer V, et al. Structural and biochemical analysis of the essential diadenylate cyclase CdaA from *Listeria monocytogenes*. *J Biol Chem.* 2015; 290: 6596–6606. <https://doi.org/10.1074/jbc.M114.630418> PMID: 25605729
24. Corrigan RM, Bowman L, Willis AR, Kaefer V, Gründling A. Cross-talk between two nucleotide-signaling pathways in *Staphylococcus aureus*. *J Biol Chem.* 2015; 290: 5826–5839. <https://doi.org/10.1074/jbc.M114.598300> PMID: 25575594
25. Oppenheimer-Shaanan Y, Wexselblatt E, Katzhendler J, Yavin E, Ben-Yehuda S. c-di-AMP reports DNA integrity during sporulation in *Bacillus subtilis*. *EMBO Rep.* 2011; 12: 594–601. <https://doi.org/10.1038/embor.2011.77> PMID: 21566650
26. Terauchi K, Ohmori M. Blue light stimulates cyanobacterial motility via a cAMP signal transduction system. *Mol Microbiol.* 2004; 52: 303–309. <https://doi.org/10.1111/j.1365-2958.2003.03980.x> PMID: 15049828

27. Diamond S, Rubin BE, Shultzaberger RK, Chen Y, Barber CD, Golden SS. Redox crisis underlies conditional light-dark lethality in cyanobacterial mutants that lack the circadian regulator, RpaA. *Proc Natl Acad Sci U S A*. 2017; 114: E580–E589. <https://doi.org/10.1073/pnas.1613078114> PMID: 28074036
28. Rubin BE, Wetmore KM, Price MN, Diamond S, Shultzaberger RK, Lowe LC, et al. The essential gene set of a photosynthetic organism. *Proc Natl Acad Sci U S A*. 2015; 201519220–201519210.
29. Welkie DG, Rubin BE, Chang Y-G, Diamond S, Rifkin SA, LiWang A, et al. Genome-wide fitness assessment during diurnal growth reveals an expanded role of the cyanobacterial circadian clock protein KaiA [Internet]. *bioRxiv*. 2018. p. 283812. <https://doi.org/10.1101/283812>
30. Allahverdiyeva Y, Mustila H, Ermakova M, Bersanini L, Richaud P, Ajlani G, et al. Flavodiiron proteins Flv1 and Flv3 enable cyanobacterial growth and photosynthesis under fluctuating light. *Proc Natl Acad Sci U S A*. 2013; 110: 4111–4116. <https://doi.org/10.1073/pnas.1221194110> PMID: 23431195
31. Shaku K, Shimakawa G, Hashiguchi M, Miyake C. Reduction-induced suppression of electron flow (RISE) in the photosynthetic electron transport system of *Synechococcus elongatus* PCC 7942. *Plant Cell Physiol*. 2015; 57: 1443–1453. <https://doi.org/10.1093/pcp/pcv198> PMID: 26707729
32. Wachi Y, Burgess JG, Iwamoto K, Yamada N. Effect of ultraviolet-A (UV-A) light on growth, photosynthetic activity and production of biopterin glucoside by the marine UV-A resistant cyanobacterium *Oscillatoria* sp. *Biochim Biophys Acta*. 1995; 1244: 165–168. PMID: 7766653
33. Matsunaga T, Burgess JG, Yamada N. An ultraviolet (UV-A) absorbing biopterin glucoside from the marine planktonic cyanobacterium *Oscillatoria* sp. *Appl Microbiol Biotechnol*. 1993; 39: 250–253.
34. Moon Y-J, Kim S, Chung Y-H. Sensing and responding to UV-A in cyanobacteria. *Int J Mol Sci*. 2012; 13: 16303–16332. <https://doi.org/10.3390/ijms131216303> PMID: 23208372
35. Sakata S, Mizusawa N, Kubota-Kawai H, Sakurai I, Wada H. Psb28 is involved in recovery of photosystem II at high temperature in *Synechocystis* sp. PCC 6803. *BBA—Bioenergetics*. 2013; 1827: 50–59. <https://doi.org/10.1016/j.bbabi.2012.10.004> PMID: 23084968
36. Finn RD, Coghill P, Eberhardt RY, Eddy SR, Mistry J, Mitchell AL, et al. The Pfam protein families database: towards a more sustainable future. *Nucleic Acids Res*. 2016; 44: D279–D285. <https://doi.org/10.1093/nar/gkv1344> PMID: 26673716
37. Cao Y, Pan Y, Huang H, Jin X, Levin EJ, Kloss B, et al. Gating of the TrkH ion channel by its associated RCK protein TrkA. *Nature*. 2013; 496: 317–322. <https://doi.org/10.1038/nature12056> PMID: 23598339
38. Moscoso JA, Schramke H, Zhang Y, Tosi T, Dehbi A, Jung K, et al. Binding of cyclic di-AMP to the *Staphylococcus aureus* sensor kinase KdpD occurs via the universal stress protein domain and down-regulates the expression of the Kdp potassium transporter. *J Bacteriol*. 2015; 198: 98–110. <https://doi.org/10.1128/JB.00480-15> PMID: 26195599
39. Corrigan RM, Campeotto I, Jeganathan T, Roelofs KG, Lee VT, Gründling A. Systematic identification of conserved bacterial c-di-AMP receptor proteins. *Proc Natl Acad Sci U S A*. 2013; 110: 9084–9089. <https://doi.org/10.1073/pnas.1300595110> PMID: 23671116
40. Roelofs KG, Wang J, Sintim HO, Lee VT. Differential radial capillary action of ligand assay for high-throughput detection of protein-metabolite interactions. *Proc Natl Acad Sci U S A*. 2011; 108: 15528–15533. <https://doi.org/10.1073/pnas.1018949108> PMID: 21876132
41. Gutu A O'Shea EK. Two antagonistic clock-regulated histidine kinases time the activation of circadian gene expression. *Mol Cell*. 2013; 50: 288–294. <https://doi.org/10.1016/j.molcel.2013.02.022> PMID: 23541768
42. Markson JS, Piechura JR, Puszyńska AM, O'Shea EK. Circadian control of global gene expression by the cyanobacterial master regulator RpaA. *Cell*. 2013; 155: 1396–1408. <https://doi.org/10.1016/j.cell.2013.11.005> PMID: 24315105
43. Diamond S, Jun D, Rubin BE, Golden SS. The circadian oscillator in *Synechococcus elongatus* controls metabolite partitioning during diurnal growth. *Proc Natl Acad Sci U S A*. 2015; 112: E1916–25. <https://doi.org/10.1073/pnas.1504576112> PMID: 25825710
44. Tsinoiremas NF, Ishiura M, Kondo T, Andersson CR, Tanaka K, Takahashi H, et al. A sigma factor that modifies the circadian expression of a subset of genes in cyanobacteria. *EMBO J*. 1996; 15: 2488–2495. PMID: 8665856
45. Sureka K, Choi PH, Precit M, Delince M, Pensinger DA, Huynh TN, et al. The cyclic dinucleotide c-di-AMP is an allosteric regulator of metabolic enzyme function. *Cell*. 2014; 158: 1389–1401. <https://doi.org/10.1016/j.cell.2014.07.046> PMID: 25215494
46. Gundlach J, Herzberg C, Kaefer V, Gunka K, Hoffmann T, Weiß M, et al. Control of potassium homeostasis is an essential function of the second messenger cyclic di-AMP in *Bacillus subtilis*. *Sci Signal*. 2017; 10. <https://doi.org/10.1126/scisignal.aal3011> PMID: 28420751
47. Hosokawa N, Hatakeyama TS, Kojima T, Kikuchi Y, Ito H, Iwasaki H. Circadian transcriptional regulation by the posttranslational oscillator without de novo clock gene expression in *Synechococcus*. *Proc*

- Natl Acad Sci U S A. 2011; 108: 15396–15401. <https://doi.org/10.1073/pnas.1019612108> PMID: 21896749
48. Ito H, Mutsuda M, Murayama Y, Tomita J, Hosokawa N, Terauchi K, et al. Cyanobacterial daily life with Kai-based circadian and diurnal genome-wide transcriptional control in *Synechococcus elongatus*. Proc Natl Acad Sci U S A. 2009; 106: 14168–14173. <https://doi.org/10.1073/pnas.0902587106> PMID: 19666549
 49. Vijayan V, Zuzow R, O'Shea EK. Oscillations in supercoiling drive circadian gene expression in cyanobacteria. Proc Natl Acad Sci U S A. 2009; 106: 22564–22568. <https://doi.org/10.1073/pnas.0912673106> PMID: 20018699
 50. Takano S, Tomita J, Sonoike K, Iwasaki H. The initiation of nocturnal dormancy in *Synechococcus* as an active process. BMC Biol. 2015; 13: 36. <https://doi.org/10.1186/s12915-015-0144-2> PMID: 26058805
 51. Puszynska AM, O'Shea EK. Switching of metabolic programs in response to light availability is an essential function of the cyanobacterial circadian output pathway. Elife. 2017; 6. <https://doi.org/10.7554/eLife.23210> PMID: 28430105
 52. Checchetto V, Segalla A, Sato Y, Bergantino E, Szabo I, Uozumi N. Involvement of potassium transport systems in the response of *Synechocystis* PCC 6803 cyanobacteria to external pH change, high-intensity light stress and heavy metal stress. Plant Cell Physiol. 2016; 57: 862–877. <https://doi.org/10.1093/pcp/pcw032> PMID: 26880819
 53. Checchetto V, Segalla A, Allore G. Thylakoid potassium channel is required for efficient photosynthesis in cyanobacteria. Proc Natl Acad Sci U S A. 2012; 109: 11043–11048. <https://doi.org/10.1073/pnas.1205960109> PMID: 22711813
 54. Price MN, Wetmore KM, Waters RJ, Callaghan M, Ray J, Kuehl JV, et al. Deep annotation of protein function across diverse bacteria from mutant phenotypes. bioRxiv. 2016;
 55. Clerico EM, Ditty JL, Golden SS. Specialized techniques for site-directed mutagenesis in cyanobacteria. Methods Mol Biol. 2007; 362: 155–171. https://doi.org/10.1007/978-1-59745-257-1_11 PMID: 17417008
 56. Chen Y, Holtman CK, Taton A, Golden SS. Functional analysis of the *Synechococcus elongatus* PCC 7942 genome. Functional genomics and evolution of photosynthetic systems. Dordrecht: Springer Netherlands; 2012. pp. 119–137.
 57. Taton A, Unglaub F, Wright NE, Zeng WY, Paz-Yepes J, Brahmasha B, et al. Broad-host-range vector system for synthetic biology and biotechnology in cyanobacteria. Nucleic Acids Res. 2014; 42: e136. <https://doi.org/10.1093/nar/gku673> PMID: 25074377
 58. Schindelin J, Rueden CT, Hiner MC, Eliceiri KW. The ImageJ ecosystem: An open platform for biomedical image analysis. Mol Reprod Dev. 2015; 82: 518–529. <https://doi.org/10.1002/mrd.22489> PMID: 26153368
 59. Moronta-Barrios F, Espinosa J, Contreras A. Negative control of cell size in the cyanobacterium *Synechococcus elongatus* PCC 7942 by the essential response regulator RpaB. FEBS Lett. 2013; 587: 504–509. <https://doi.org/10.1016/j.febslet.2013.01.023> PMID: 23340342
 60. Team RC. R: A language and environment for statistical computing. R Foundation for Statistical Computing, Vienna, Austria. 2013. 2014.
 61. Benjamini Y, Hochberg Y. Controlling the false discovery rate: a practical and powerful approach to multiple testing. J R Stat Soc Series B Stat Methodol. JSTOR; 1995; Available: <http://www.jstor.org/stable/2346101>